Arabian Journal for Science and Engineering (2023) 48:205–222
https://doi.org/10.1007/s13369-022-06856-9

RESEARCH ARTICLE-CHEMISTRY

Electrospun PVA–Dextran Nanofibrous Scaffolds for Acceleration of Topical Wound Healing: Nanofiber Optimization, Characterization and In Vitro Assessment

El-Refaie S. Kenawy[1] · Elbadawy A. Kamoun[2,3] · Mahmoud Serag Eldin[1] · Hesham M. A. Soliman[4] · Shahira H. EL-Moslamy[5] · Esmail M. El-Fakharany[6] · Abdel-baset M. Shokr[1]

Received: 6 September 2021 / Accepted: 29 March 2022 / Published online: 30 May 2022

Abstract

Electrospun polyvinyl alcohol–dextran (PVA–Dex)-based nanofibers (NFs) are explored as a novel class of bioactive injury dressing materials, which have an essential role for topical injury mending. Sodium ampicillin-loaded citric acid-cross-linked PVA–Dex NFs were fabricated by electrospinner for wound recuperating purposes. Results revealed that PVA (10%)–dextran (10%) cross-linked with 5% citric acid (CA) was chosen as an optimized condition for obtaining non-beaded and morphological accepted nanofibers. Altered concentrations of CA as cross-linker progressively enhanced significantly the mechanical/thermal stability and wettability-proof of NFs scaffolds, compared to un-cross-linked (PVA–Dex) scaffolds. Meanwhile, swelling (%), protein adsorption and released ampicillin of NFs decreased dramatically with the increase in the CA concentration, and conversely enhanced with increasing dextran concentrations. Interestingly, resultant PVA–Dex NFs with high concentrations of dextran promoted the proliferation of *HFB-4* cells in a high concentration-dependent manner and high antimicrobial activity behavior, compared to NFs containing high concentrations of CA cross-linker after 24 and 48 h of cell exposure. Notably, all fabricated NFs have remarked ability to accelerate the rate of in vitro wound gap closure (%) after treatment for 24 and 48 h, compared to control sample. However, reducing CA concentration in NFs showed the highest percentages of wound healing for scratched *HFB-4* cells with clear observed healing process.

Keywords PVA/dextran nanofiber · Electrospinning · Bioevaluation assessments

1 Introduction

A wound is an injury in which the dermal area is damaged, due to a cut or defected part. Generally, wounds are divided into two types, known as acute and chronic wounds. Chronic wounds display prolonged and abnormal inflammation, regular infections, presence of resistant microbial biofilms and failure of dermal and epidermal cells that return to repair stimuli. Acute wounds follow a predictable, well-controlled

✉ El-Refaie S. Kenawy
ekenawy@yahoo.com

✉ Elbadawy A. Kamoun
e-b.kamoun@tu-bs.de

[1] Polymer Research Group, Department of Chemistry, Faculty of Science, University of Tanta, Tanta 31527, Egypt

[2] Nanotechnology Research Center (NTRC), The British University in Egypt (BUE), El-Sherouk City, Cairo 11837, Egypt

[3] Polymeric Materials Research Department, Advanced Technology and New Materials Research Institute (ATNMRI), City of Scientific Research and Technological Applications (SRTA-City), New Borg Al-Arab City, Alexandria 21934, Egypt

[4] Nanotechnology and Composite Materials Department, Advanced Technology and New Materials Research (ATNMRI), City of Scientific Research and Technological Applications (SRTA-City), New Borg Al-Arab City, Alexandria 21934, Egypt

[5] Bioprocess Development Department, Genetic Engineering and Biotechnology Research Institute (GEBRI), City of Scientific Research and Technological Applications (SRTA-City), New Borg Al-Arab City, Alexandria 21934, Egypt

[6] Protein Research Department, Genetic Engineering and Biotechnology Research Institute (GEBRI), City of Scientific Research and Technological Applications (SRTA-City), New Borg Al-Arab City, Alexandria 21934, Egypt

process, including platelets, fibroblasts, keratinocytes and immune surveillance cells. Previous studies emphasized that wound valuation is the most critical step, diagnosis and treatment of wounds [1]. Wound healing of acute and chronic skin injuries is a quite complex process, and today's handlings face huge trials in clinical repetition. One of the basic medical methods to treat chronic wounds is to use proper topical dressings with extraordinary characteristics to promote the healing of wounds [1–3].

Hitherto, analysts have zeroed in on creating present day NF-based dressings that could imitate the local dermal extracellular framework (ECM) and have the function of setting up and keeping up an ideal climate for wound fix [4]. These nanofibers can deliver dynamic substances. For example, normal or manufactured antimicrobials or various operators with inborn bacteriostatic or potentially bactericidal movement are ready to invigorate the recuperating cycle. For a compelling plan of a practical injury dressing, convinced highlights must be satisfied, e.g., injury type, wound mending time, physical, mechanical and synthetic properties of the framework are significant elements [1, 5–7]. An ideal injury dressing ought to give bacterial insurance that permits liquid trades, a soggy climate (eliminating abundance exudate) and ideal recuperating climate, be non-harmful, non-allergenic and savvy [8, 9], biocompatible with no dismissal and additional irritation, and help quicken re-epithelialization. The permeable engineering ought to be interconnected for the transportation of oxygen and supplements and a decent cell grip ought to be encouraged by having an enormous surface zone [10, 11]. Likewise, a decent quality of the dressing is needed because of its different mechanical mishappenings and dynamic loadings [12]. So, as to get such appropriate dressing materials, both the biomaterial arrangement and the preparing innovation assume significant jobs. In this manner, biomaterials, for example, characteristic polymers (collagen, chitosan, keratin and so forth) or engineered biomaterials, e.g., PLA, PEO, PCL, PLG) and so on, could be appropriate dressings for skin recovery [12, 13].

As of late, the plan and creation of novel bioactive nanofibrous mats by means of electrospinning (easy fabrication, produces continuous and homogeneous nanofibers, and cost-effective technique producing an assortment of polymeric 3D frameworks for fake body tissue implantation or different applications) have pulled in more consideration [14–16]. The tale electrospun NFs should act like a viable physical hindrance that shields the exposed injury from additional pollution with exogenous microbes [17, 18]. Electrospinning procedure is a straightforward and adaptable cycle for planning filaments having a measurement from not many micrometers down to a few nanometers [19, 20]. The subsequent NFs have exceptional highlights, for example, high surface territory to volume proportion, and can frame mats/wools with high permeability which makes them appealing materials for versatile medical dressings [21, 22]. Lately, electrospun sinewy frameworks copy the structure of the local extracellular lattice (ECM) and thus encourage cell expansion, improve vaporous trade and expulsion of exudates, and go about as a physical hindrance against passage of microbes during wound mending and recovery of defected tissues [21, 23–26].

Biomaterial-based polymeric nanofibers (NFs) were produced using biodegradable and biocompatible manufactured or natural polymers and have been used to create drug conveyance frameworks to treat different afflictions. One of the expected zones to utilize them is sedated wound dressing [21, 23]. PVA is a biocompatible/biodegradable hydrophilic polymer with great synthetic and mechanical strength, and it has been affirmed by USFDA for various biomedical and drug applications [27, 28]. Furthermore, PVA was wide utilized to produce hydrogels for wound dressing [29] or electrospun along with dynamic substances, for example, silver NPs [30] and curcumin [31], to deliver wound dressings. PVA nanofibers were blended previously with other polymers like PVA/sodium alginate (SA) [32, 33], PVA/starch and hydroxyethyl starch (HES) [34, 35], PVA/glucan [36], PVA/chitosan and dextran [37, 38] and PVA/gelatin (GE) [39] for versatile biomedical applications [40–42].

Dextran is a bacterial linear polysaccharide, which composes of α-1, 6-connected *D*-glucopyranose residues with low level of α-1,2, α-1,3 and α-1,4 connected side chains [41]. Dextran is extracted from *Leuconostoc mesenteroides* contains around 5% of α-1,3-glycopyranosidic linkages, which are generally a couple of glucose buildups long. In the past years, dextran was used as one of the broadest utilized blood plasma expanders. As a result of its great biocompatibility and biodegradability, it is likewise an appropriate candidate for hydrogels production [37, 42–44], which zeroed in on accomplishing a steadier and glasslike truly cross-linked PVA/Dex hydrogel membranes utilizing freezing–defrosting strategy. This early investigation demonstrated that the presence of dextran in PVA framework favors the crystallization cycle of PVA, permitting the arrangement of a more arranged and regular PVA hydrogel networks. PVA/Dex membranes demonstrated brilliant arranged structure contrasted with PVA mixed with chitosan. Generally, PVA/Dex hydrogel membranes demonstrated greater swelling % and fairly high delivery profile of delivered free-PVA, contrasted with PVA/chitosan hydrogel membranes. Also, gentamicin-loaded PVA/Dex hydrogel membranes were designed by Hwang et al. [45]. The freezing–drying technique has been utilized for genuinely physical cross-linking of PVA/Dex hydrogel membranes. Gentamicin-loaded physically cross-linked PVA/Dex hydrogel membranes essentially improved the injury recuperating, wound size decrease and spots on rodent dorsum contrasted with the free drug PVA/Dex hydrogel layers in view of the expected mending impact of gentamicin. However, no previous study introduced a detailed

discussion for optimization electrospinning conditions of fabricated ampicillin-loaded CA-cross-linked PVA–dextran nanofibers for topical wound dressing and assessing their applicability as scaffolds [29, 40].

This study aims to fabricate and optimize electrospun nanofibrous scaffolds composed of ampicillin-loaded CA-cross-linked (PVA/Dex) NFs using electrospinner as potential platform for topical wound dressing applications. CA was utilized as a non-toxic chemical cross-linker to offer accepted mechanically electrospun (PVA/Dex) NFs with suitable waterproof and vigorous to several biomedical demands. The impact of dextran and citric acid in addition to PVA nanofibers was intensively studied and estimated in terms of the whole physicochemical properties, cell viability, antimicrobial activity and in vitro wound closure (%) of electrospun PVA/Dex NFs mats.

2 Materials and Methods

2.1 Materials

Polyvinyl alcohol (PVA) (95.5–96.5% hydrolyzed, $M._{wt}$ ~ 85,000 − 124,000 g/mol) was purchased from ACROS, USA. Dextran (Dex) from *Leuconostoc sp.* $M._{wt}$ approx. 40,000 g/mol was purchased from Sigma-Aldrich, USA. Citric acid (CA) was purchased from (Riedel-deHaën, Germany). Ampicillin sodium salt and bovine serum albumin (BSA) were purchased from Sigma-Aldrich Chemie GmbH, Steinheim, Germany.

2.2 Fabrication of Electrospun PVA–Dextran Nanofibers

PVA was dissolved in distilled water in varied concentrations ranged as 5, 10 and 15% w/v in 10 ml distilled water; PVA solutions were then electrospun into nanofibers at different applied voltages as shown in Table 1 and Table 1, supplementary data, for determining the proper PVA concentration which produces non-bead nanofibers. Each electrospinning process was conducted at room temperature with RH ≤ 55%. Also, dextran was dissolved in distilled water in ranged concentrations from 50, 70, 90 and 110% w/v, and the PVA/Dex solutions were then electrospun into NFs at different applied voltages as shown in Table 2, supplementary data, for choosing the proper dextran concentration for further attempts of NFs fabrication with accepted mats morphology.

Different ratios of PVA–dextran solutions were then mixed with different concentrations of CA as chemical cross-linker as ranged 0, 1, 3, 5 and 10, w/w, and the obtained mixture solutions were then electrospun into NFs at altered voltages as shown in Tables 3 and 4, supplementary data.

2.3 Spinning Condition Optimization of Electrospun CA-Cross-linked PVA–Dextran NFs

A 9 ml of PVA (10%, w/v) was mixed with one ml of Dex (10%, w/v), and then, PVA–Dex solution was retained under agitation for 24 h at ambient conditions. CA (5% w/w) was mixed to PVA–Dex solution, and then, the mixture solution was kept under stirring for further one hour at room temperature, followed by ultra-mixing in an ultrasonic water bath for 30 min at ambient conditions before electrospinning, for guarantee the homogeneity of polymer–CA mixture solution. The polymeric mixture was electrospun at applied power voltage of 27 kV from a high voltage source (Gamma high voltage research, Inc., FL, USA), at 55% humidity, using electrospinner (model Nano-NC, South Korea). The formed NFs were collected over static plate collector kept at 10 cm from the needle, while the feeding solution rate was reserved at 0.5 ml/h [46–48]. The scaffolds were collected on sheets of aluminum foil, dried under vacuum at 80 °C for overnight to eliminate the residual solvent and to complete the esterification reaction, and kept in a dry/cold condition to prevent any possible contaminations. Sodium ampicillin (100 mg) was loaded to CA-cross-linked PVA–Dex mixture solution before electrospinning for determination of the profile control released sodium ampicillin from NFs.

2.4 Instrumental Characterization of CA-Cross-linked (PVA–Dex) NFs

PVA/Dex NFs were instrumentally analyzed by FTIR, SEM, TGA and tensile strength, as shown in *Supplementary data*.

2.5 Physicochemical Measurements of CA-Cross-linked PVA–Dex NFs

2.5.1 Surface Wettability

The surface wettability of NFs was defined by static water contact angle model (DSA30, Krüss GmbH, Hamburg, Germany). The data were collected by DSA image analysis software (DSA4.2.0. Krüss GmbH, Hamburg, Germany). The sample of NFs was fixed onto glass-side, the water was dropped onto sample surface using syringe needle and the contact angle values were measured at zero time (i.e., when the water drop contacts the surface suddenly).

2.5.2 Moisture Uptake (%)

AN exactly weighed of NFs specimen (9 cm^2) of cross-linked CA-(PVA–Dex) NFs was located in a *Petri* dish and attached in a desiccator filled with water. After 48 h, NFs

Table 1 Electrospun nanofiber samples codes and their corresponding composition and optimization

Sample codes	PVA (wt%)	Dextran (wt%)	CA (wt%)	(PVA:Dex) ratio	Purpose
M_1	5	0	0	–	Optimization of PVA NFs. Un-cross-linked NFs
M_2	7	0	0	–	
M_3	10	0	0	–	
M_4	15	0	0	–	
M_5	0	50	0	–	Optimization of dextran NFs. Un-cross-linked NFs
M_6	0	70	0	–	
M_7	0	90	0	–	
M_8	0	110	0	–	
M_9	10	90		9:1	Optimization of CA-cross-linked PVA–Dex NFs
M_{10}	10	90		8:2	
M_{11}	10	90		7:3	
M_{12}	10	40	5	9:1	Optimization of ratio of PVA–Dex. cross-linked NFs
M_{13}	10	40	5	8:2	
M_{14}	10	40	5	7:3	
M_{15}	10	50	5	9:1	Optimization of dextran concentration in cross-linked PVA–Dex NFs
M_{16}	10	30	5	9:1	
M_{17}	10	20	5	9:1	
M_{18}	10	10	0	9:1	
M_{19}	10	10	1	9:1	Optimization of CA concentration in PVA–Dex NFs
M_{20}	10	10	3	9:1	
M_{21}	10	10	5	9:1	
M_{22}	10	10	10	9:1	
M_{23}	10	10	5	9:1	
M_{24}	10	10	5	9:1	

were reweighed again for calculating moisture uptake %, as given equation [3, 29]:

$$\text{Moisture uptake}\,(\%) = (W_s - W_0)/W_0 \times 100. \quad (1)$$

where W_s is the weight of the swollen NF and W_0 is the weight of the original NF.

2.5.3 Swelling Index

CA-(PVA–Dex) NFs were weighed (W_1) and soaked in a *Petri dish* containing PBS, pH 6.8. After 5 min., NFs were reisolated and the additional water was dried by a fine paper. The swollen films were reweighed (W_2) at time intervals against the sample weight change, as shown in Eq. (2) [29, 40].

$$\text{Swelling index, SI} = (W_2 - W_1)/W_1. \quad (2)$$

2.5.4 Protein Adsorption Study

The amount of adsorbed bovine serum albumin (BSA) onto NFs outer surfaces was detected by UV–Vis spectrophotometer at 630 nm (Agilent technologies, Cary series UV–Vis–NIR, Korea) with supporting a standard calibration curve of BSA ranging from 3 to 60 mg ml^{-1}. Beer's law was used to determine the exact adsorbed BSA at NFs surfaces. Pieces of three types of NFs were cut into 1 cm × 1 cm, then were immersed in 10 ml PBS (pH 7.4) and incubated at 37 °C for 24 h until reach to equilibrium swelling weight. The swollen NFs scaffolds were transferred to buffer solution containing BSA (30 mg ml^{-1}) and shacked for 4 h at 37 °C, and then, NFs pieces were gently removed. The protein adsorption was calculated by the difference between protein concentrations before/after immersing NFs pieces in BSA/PBS using albumin reagent kit at 630 nm [29].

2.5.5 Drug Release Study

The profile released sodium ampicillin from CA-cross-linked PVA–Dex NFs scaffolds as a function of different CA cross-linker concentrations was determined by membrane diffusion method. A 100 mg of sodium ampicillin was dissolved in CA-PVA–Dex at room temperature directly before spinning step. Full sheet of NFs was soaked in 10 ml of phosphate buffer pH ~ 7 as a release medium at 37 °C. At interval times, the concentration of released ampicillin was measured by spectrophotometer model (Agilent Tech., Cary Series UV–Vis–NIR, South Korea) at 275 nm. The concentration of released ampicillin from NFs was calculated based on an ampicillin standard curve. Released ampicillin % was assessed as the given equation [29, 40].

$$\text{Release}\,(\%) = \text{Released ampicillin}/\text{Total ampicillin} \times 100. \quad (3)$$

2.6 In Vitro Bioevaluation Tests

2.6.1 Antimicrobial Activity of CA-PVA/Dex Nanofiber Scaffolds

- *Antagonistic efficiency for formulated hydrogel disks in vitro*

The formulated hydrogels coded as G1 (10% PVA: 10% dextran: 5% CA), G2 (10% PVA: 5% dextran: 5% CA), G3 (10% PVA: 20% dextran: 5% CA), G4 (10% PVA: 10% dextran: 1% CA), G5 (10% PVA: 10% dextran: 3% CA) and G6 (10% PVA: 10% dextran: 10% CA) were tested in terms of their resistance for microbial growth. Furthermore, used multidrug-resistant human pathogens were obtained from Bioprocess Development Dep., GEBRI, SRTA-City, Egypt. Thus, the antagonistic effects were determined statistically by performing the following steps:

- *Media preparation*

In this test, the nutrient agar (NA) and Mueller–Hinton agar (MHA) media were employed for bacterial and fungal pathogens, respectively. Thus, the NA medium (Sigma-Aldrich) was composed of 0.1% meat extract, 0.5% peptone, 0.2% yeast extract, 0.5% NaCl, 1.5% agar, while pH was adjusted at 6.8 ± 0.5. Besides, the MHA medium (Sigma-Aldrich, Germany) consisted of 0.2% beef infusion solids, 1.8% casein hydrolysate, 0.2% starch and 1.7% agar. Media was prepared using distilled water and sterilized by autoclaving at 120 °C for 25 min.

- *Preparation of multidrug-resistant human pathogens*

The most important pathogens that caused the skin and soft tissue infections such as *Staphylococcus aureus* (*gram-positive* bacteria), *Streptococcus pyogenes* (*gram-positive* bacteria), *Pseudomonas aeruginosa* (*gram-negative* bacteria), *Klebsiella pneumoniae* (*gram-negative* bacteria) and *Candida albicans* (fungal cells) were selected to calculate the antagonistic activities in this study. Thus, the preserved bacterial and fungal cells were stroked on NA plates and MHA plates, respectively. Subsequently, these plates were incubated at 30 °C for 48 h.

- *Inoculums preparation*

The nutrient broth (NB) medium was prepared by using the following ingredients: 0.1% meat extract, 0.5% peptone, 0.2% yeast extract and 0.5% NaCl, and the final pH was adjusted at 6.8 ± 0.5. Moreover, the Mueller–Hinton broth (MHB) medium was prepared by dissolving 0.2 g beef infusion solids, 1.8 g casein hydrolysate and 0.2 g starch in 100 ml distilled water, and the final pH was adjusted approximately at 7.0 ± 0.5. Subsequently, the single colonies of these human pathogens were selected and inoculated into 500-ml shake flasks that contained about 100 ml of each broth media that used for bacterial and fungal cells individually. Then, these flasks were incubated using a shaking incubator at 250 rpm, 30 °C, for 24 h. Finally, these cultures were used as inoculums in the following steps.

- *Antagonistic activities assay*

The disk diffusion method was applied to assess the antimicrobial efficiency in this study. Thus, the prepared microbial cultures were diluted to 0.5 McFarland standards using serial NaCl solution (0.9%). Then, the prepared MHA plates were swabbed with 100 µl of the *Candida albicans* dilution but other the tested bacterial dilutions were inoculated individually on NA plates (100 µl/plate). After the diffusion period (3 h at 4 °C), the tested membranes were prepared as disks (5 mm) and employed on the surface of inoculated agar plates. Triplicates were conducted for each pathogen. These plates were incubated statically at 30 °C for 48 h. Then, the formed inhibition/clear zones were detected in a millimeter (mm) using a centimeter roller.

2.6.2 Cytotoxicity Assay

Effect of CA-cross-linked (PVA–Dex) NFs on cell viability of *HFB-4* (human normal melanocytes) normal cell line after treatment was evaluated using MTT cell viability assay as previously defined by Mosmann (1983) and Almahdy et al., (2011) [49, 50]. In brief, *HFB-4 cells* (1.0×10^3) were seeded in triplicates in 24-well sterile flat-bottomed tissue culture micro-plate. Then, *HFB-4* cells were cultured

in DMEM (Lonza, USA) supplemented with 10% of fetal bovine serum (FBS); then, cells were incubated at 37 °C in 5% CO_2 incubator for 24 h. Then, disks of (PVA–Dex) NFs at weights of 0.25, 0.5, 1.0 and 2.0 mg/ml were added to cells in triplicates and incubated at 37 °C in 5% CO_2 incubator. After incubation for 24 and 48 h, (PVA–Dex) NFs were removed and cells were washed three times with 1.0 M of PBS to remove debris and dead cells. Then, 1.0 ml of MTT solution (0.5 mg/ml) was added to each well and incubated at 37 °C and 5% CO_2 for about 3–5 h. The formazan crystals were dissolved in 1.0 ml/well of DMSO, and the absorbance was measured at 630 nm and subtracted from measuring at 570 nm using reader a micro-plate ELISA reader. The relative cell viability (%) compared to control wells containing cells without adding (PVA–Dex) NFs disks was premeditated using the following formula: (A) test/ (A) control × 100%.

2.6.3 Cell Healing Assay

Cell healing effect of (PVA–Dex) NFs was investigated by a wound healing protocol as reported earlier by Preet et al. [51] and El-Lakany et al. [52]. Briefly, normal human melanocytes (HFB-4 cells) were seeded in 12-well cell culture plates at count of 1.0×10^5 per well and incubated in 5% CO_2, to become around 90% confluence; then, in vitro wound scratches were created by sterile micro-tips in the cell monolayer. After washing the cells with fresh media to remove the dead cells and debris, (PVA–Dex) NFs disks at weights of 0.5 and 1.0 mg/disk were added to wells, separately. After incubated in 5% CO_2 and 37 °C to allow cells to migrate in the medium for 24 and 48 h, wound healing was evaluated using phase-contrast microscope, as compared with untreated scratched cells.

2.7 Statistical Analysis

The final data were assessed statistically *via* analysis of variance by using 2017 Minitab version 18.1 Inc., for distinguish significant differences among replicates. Thus, a significant and no significant difference were demonstrated at $P < 0.05$ and $P > 0.05$, respectively.

3 Results and Discussion

3.1 Optimization of CA-Cross-linked PVA–Dex NFs Scaffolds

For optimizing PVA NFs mats, optimization of spinning conditions was carried out to fabricate morphologically accepted PVA NFs without droplet or bead formation during the spinning process, where the effects of PVA concentrations of 5, 7, 10 and 15%, w/w, spinning volume rate (0.3–0.4 ml/h), voltage (24–26 Kv) and trip-to-target distance at ~ 20 cm were tested on PVA NFs morphology and are displayed in Table 1 and Table 1, supplementary data. As seen in SEM investigation, 10%, w/w of PVA concentration was chosen for further experiments as the proper polymer concentration for NFs fabrication without beads or droplets formation.

For optimizing dextran NFs scaffolds, the spinning condition optimization were accompanied to fabricate morphologically accepted dextran NFs without droplets creation during the spinning process, where the effects of dextran concentrations of 5, 70, 90 and 110%, w/w, spinning volume rate (0.15–0.25 ml/h), applied voltage (23–24 Kv) and trip-to-target distance (20 cm) was studied and is shown in Table 2, supplementary materials. A 90% (w/w) of dextran was chosen as the suitable concentration for blending with PVA in the further experiments due to no beads formed during the spinning process. Different CA concentrations of 1, 3, 5 and 10%, w/w as cross-linker were tested for cross-linking PVA–Dex NFs ratio of 9:1 with concentration(10%:10% as shown in Table 3, supplementary materials. The moderated concentrations of CA of, i.e., 3 and 5%, w/w, showed adequate cross-linked PVA–Dex NFs, compared to other CA concentrations of 1 and 10%, w/w.

For optimizing blending conditions of spinning of electrospun cross-linked PVA–dextran NFs, with varied ratios of PVA to Dex of 9:1, 8:2 and 7:3 and different concentrations of 10:10, 10:20, 10:30, 10:40, 10:50 and 10:90 w/w, feeding rate (0.15–0.25 ml/h), applied voltage (24–29 Kv) and trip-to-target distance (20 cm) with 5%, w/w of CA for all samples, were studied and their SEM photographs are displayed in Table 4, supplementary materials. It was observed that the ratio of PVA to Dex (9:1) with concentrations of 10:10, 10:20 and 10:40, % showed morphologically accepted NFs with no beads or droplets formed during the spinning process.

3.2 Characterization of CA-Cross-linked PVA–Dex NFs Scaffolds

- *FTIR analysis*

FTIR spectra of PVA, dextran and un-cross-linked PVA–Dex scaffold (M_{18}) showed characteristic peaks at ν 3325, 3400 and 3315 cm^{-1} associated with stretching of -OH groups of alcohol, respectively. Spectrum of CA was detected at characteristic peaks at ν 1720, 1705, 1690 and 1710 cm^{-1} which are corresponding to vibration peaks of C=O bond of aliphatic ester in cross-linked (PVA/Dex) scaffolds of M_{19}–M_{24} (Table 3, *supplementary materials*), which guarantee creation of chemical bonding between (PVA–Dex)

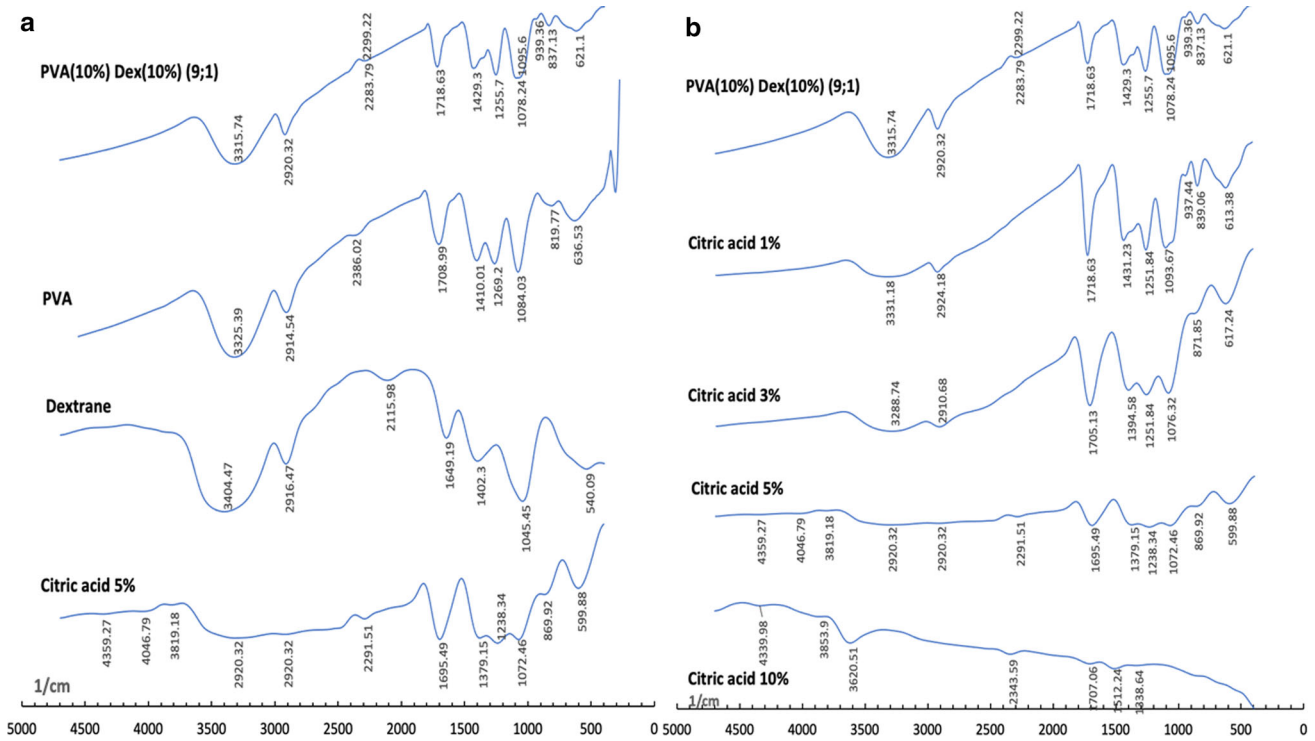

Fig. 1 FTIR spectra of **a:** PVA, dextran and selected un-cross-linked PVA–Dex NFs and **b**: CA-cross-linked PVA–Dex NFs with different CA concentrations (1, 3, 5 and 10%, w/w) (sample codes M_{19}-M_{24})

and CA resulting in CA-cross-linked PVA/Dex NFs via transesterification reaction post-heat treatment as mentioned in Sect. 2.3 (Fig. 1).

- *SEM investigation*

SEM images showed the surface morphology alteration of certain fabricated (PVA–Dex) NFs with/without CA cross-linking; images are presented in Fig. 2. The mean diameters of all NFs were analyzed using (*ImageJ, version 1.4.3*) software, which varied from 60 to 120 nm (Table 5, *supplementary data*). SEM images exhibited irregular and sphere-shaped beaded surface structures, which were obtained with high dextran concentration (M_{23}; 20%, w/v). However, decreasing dextran concentration to 10%, as w/v (M_{21}) resulted in NFs with a diameter of ~ 70 nm and a pointedly reduced amounts of produced beads. Also, decreasing dextran concentration to 5.0% (w/v) in M_{24} resulted in NFs with a diameter of ~ 120 nm and expressively reduced bead amounts were observed. The optimized un-cross-linked (PVA–Dex) scaffold as (M_{18}) was achieved, when 10% (w/v) dextran solution was employed. The impact of the applied electrospinning voltage was studied as an effective parameter during spinning process, as displayed in Fig. 2. These results are agreed with published results of Jiang et al., [53]. Similarly, growing the spinning voltage from 22 kV in NFs of M_{23} to 24 and 28 kV in NFs of M_{18}, expressively diminished the formation of beads and altered the surface morphology from ribbonlike to filamentous and uniform shape structure NFs, respectively.

In case of cross-linked CA-(PVA–Dex) NFs scaffolds, (PVA–Dex) was allowed to react with CA (1, 3, 5 and 10%, w/w) in water before electrospinning, where the average diameters of CA-PVA/Dex scaffolds, as listed in Table 5, *supplementary data* (NFs codes of M_{19}, M_{20}, M_{21} and M_{24}), which ranged from ~ 60 to120 nm.

3.3 Physicochemical Measurements of CA-Cross-linked PVA/Dex NFs

3.3.1 Mechanical Stability of NFs

Un-cross-linked (PVA–Dex) NFs showed very weak mechanical stability and a very loose/flexible shape structure was observed, owing to lack of cross-linker degree. Different concentrations of CA as chemical cross-linker progressively enhanced mechanical strength of NFs, compared to un-cross-linked (PVA–Dex) NFs. Meanwhile, NFs scaffolds of M_{22} (10%, w/w CA) exhibited the highest tensile strength of ~ 4.95 MPa, compared to low CA-cross-linked samples of M_{19} (1%, w/w of CA), M_{20} (3% w/w CA) M_{21} (5%, w/w of CA), M_{23} (5%, w/w of CA and Dex 20%, w/w) and M_{24} (5%, w/w of CA and Dex 5%, w/w), which presented tensile strength of 0.62, 2.65, 4.5, 3.8 and 4.5 MPa, respectively (Table 2).

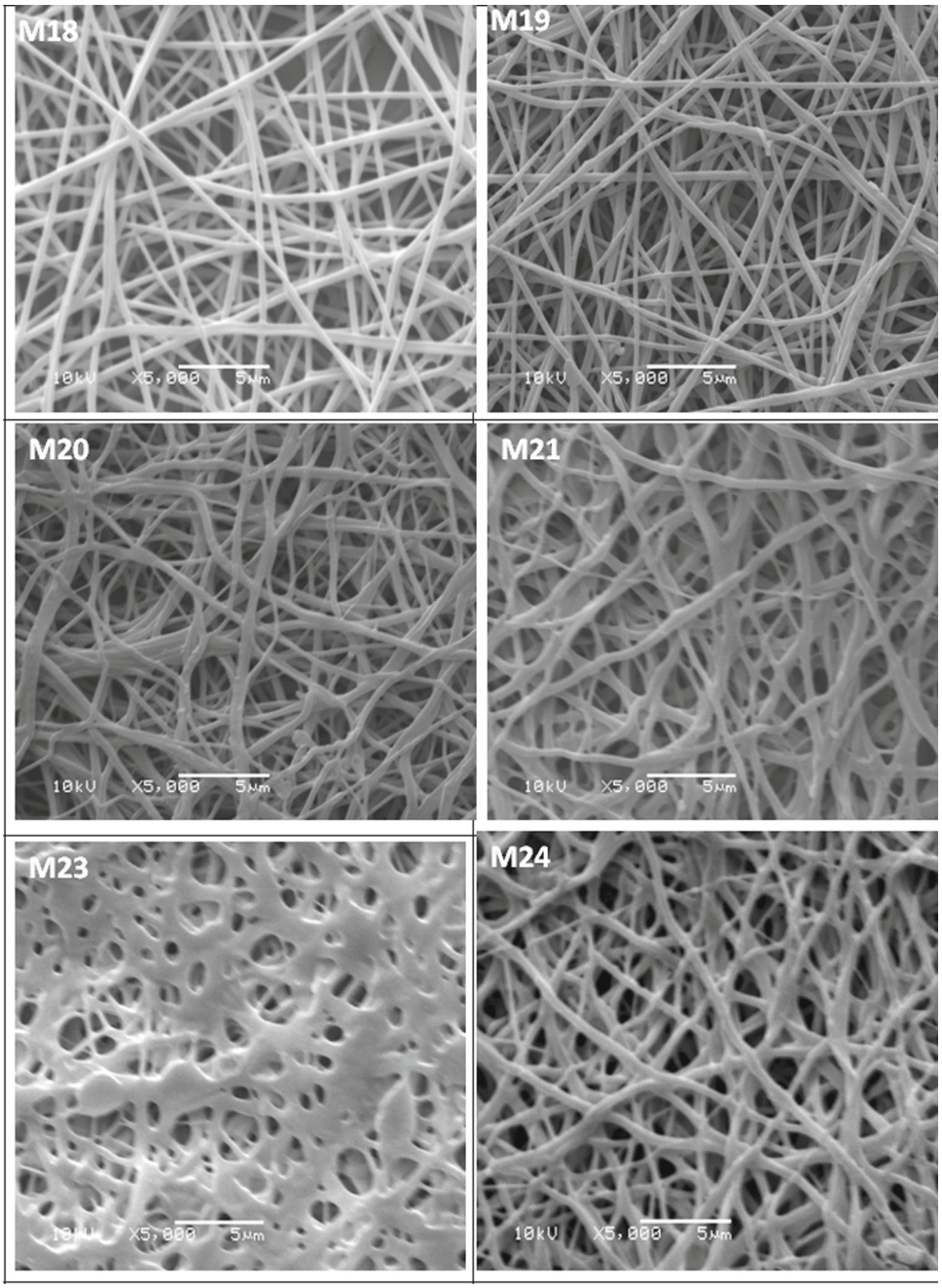

Fig. 2 SEM images of selected (PVA–Dex) nanofibrous scaffolds; un-cross-linked NFs (M_{18}), cross-linked NFs (M_{19}, M_{20}–M_{24}) (all images were investigated at original magnification × 5000 @ 10 kV and scale bar 5 μm)

The mechanical stability behavior could be elucidated by formation of ester linkages between CA cross-linker and (PVA–Dex), where the cross-linking process enriched the inter-connective structure between molecules, and therefore minimized their slippage during tensile testing. It is shown that increasing concentration of CA as a cross-linker in NFs improved significantly tensile strength. On the contrary, increasing Dex concentration (20% Dex w/w) in NFs showed a clear decrease in the tensile strength (3.8 MPa) (Table 2). This behavior was explained by the fact that dextran is a very high hydrophilic polymer, while high portion of dextran might result in mechanical strength deterioration. However, the increase in the CA cross-linker concentration enhanced obviously the mechanical stability of NFs, owing to increasing the cross-linking degree and density forming tight and compressed interconnected NFs.

3.3.2 Thermal Stability of NFs by TGA

TGA thermographs of NFs were achieved to examine the influence of CA cross-linker concentration in mats on thermal decomposition behavior of CA-(PVA/Dex) NFs scaffolds.

Table 2 Mechanical properties of electrospun CA-cross-linked (PVA/Dx) NFs as a function of different concentrations of CA as cross-linker and dextran

Sample code	NFs composition	Elongation to break (%)	Tensile strength (MPa)	Elastic modulus (MPa)
M_{19}	1 (w/w, %) CA	3.98 ± 0.25	0.62 ± 0.15	28 ± 4.23
M_{20}	3 (w/w, %) CA	5.25 ± 0.35	2.65 ± 0.31	69 ± 5.11
M_{21}	5 (w/w, %) CA	9.25 ± 0.97	4.5 ± 0.56	111 ± 4.25
M_{22}	10 (w/w, %) CA	7.25 ± 0.22	4.95 ± 0.29	146 ± 1.29
M_{23}	5 (w/w, %) CA 20 (w/w, %) Dex	18.5 ± 0.98	3.8 ± 1.0	95 ± 2.12
M_{24}	5 (w/w, %) CA 5 (w/w, %) Dex	14.25 ± 1.1	4.1 ± 0.65	98 ± 3.25

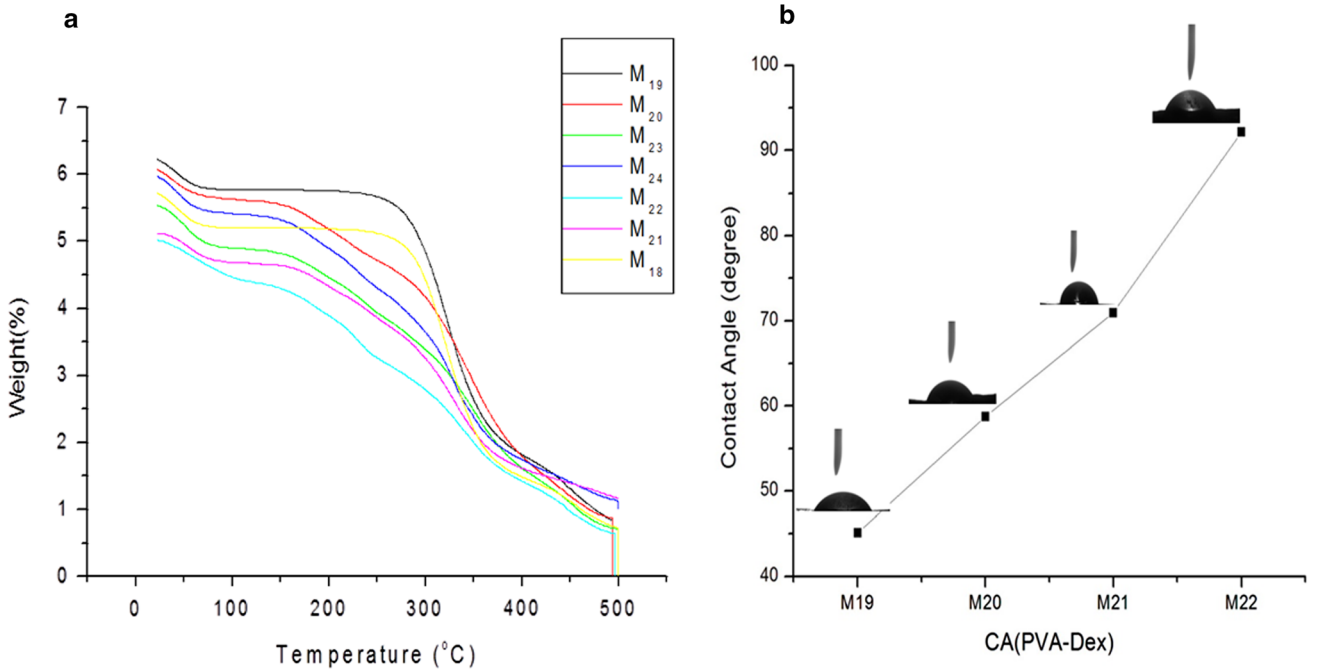

Fig. 3 **a** TGA thermograph curves of un-cross-linked and CA-cross-linked (PVA–Dex) NFs scaffolds, as a function of different CA cross-linker concentrations; **b** contact angle measurements of CA-cross-linked (PVA–Dex) NFs as a function of different CA concentrations and different NFs compositions

TGA thermographs of all (PVA/Dex) scaffolds are displayed in Fig. 3a, whereas TGA data are listed in Table 3. The first degradation stage in thermograph displayed a higher moisture absorption in all samples of (PVA/Dex) NFs (M_{19}–M_{24}), compared to original un-cross-linked (PVA/Dex) NFs of M_{18} as a result of the removal of moisture in (PVA–Dex) NFs mats (≤ 100 °C). The 2nd degradation stage of graphs demonstrated the thermal degradation onset (T_{onst}), and the temperature at 50% weight loss increased gradually of NFs codes of M_{18} and M_{20} *ca.* from 238 to 301 °C and from 379 to 400 °C, respectively, owing to increasing the cross-linking degree of cross-linked NFs caused by CA concentration increase (Table 3). As expectedly, the increase in the portion of dextran concentration from 5 to 20% (w/w) decreased sharply the thermal stability of the 2nd degradation stages onset from 300 to 242 °C. Interestingly, current results are matching with obtained results of mechanical stability, as shown in Table 2. This implies that both mechanical and thermal stability of cross-linked NFs increased notably as a function of CA concentration increases and they decreased significantly with increasing the dextran contents in NFs.

Table 3 Thermal stability data of un-cross-linked and cross-linked CA-(PVA–Dex) NFs adapted from TGA thermographs

Sample code	NFs composition	T_{onset} (°C)	50% Weight loss at Temp. (°C)	1st decomposition stage °C, (weight loss, %)	2nd decomposition stage (°C) (weight loss, %)
M_{18}	0 (%, w/w) CA	238	380	100–2645 (3%)	264.88–499.9 (75.4%)
M_{19}	1 (%, w/w) CA	265	382	76–238 (1.5%)	237.86–499.9 (78.1%)
M_{20}	3 (%, w/w) CA	301	400	101–301 (23%)	300.86–499.9 (55.27%)
M_{21}	5 (%, w/w) CA	200	341	101–200 (8%)	200.28–499.9 (61.32%)
M_{22}	10 (%, w/w) CA	300	400	100–300 (33%)	299.84–500 (43.66%)
M_{23}	5 (%, w/w) CA 20 (%, w/w) Dex	243	351	100–242 (16%)	242.23–499.9 (59.64%)
M_{24}	5 (w/w, %) CA 5 (%, w/w) Dex	300	341	101–300 (30%)	300.36–499.9 (42.01%)

3.3.3 Surface Wettability of NFs

Basically, the surface wettability of NFs seriously affects the protein adsorption and cell adhesion of biomaterials; thus, the value of the contact angle gives insights into the degree of surface wettability upon the contact between biomaterial surface and biological fluids [52]. It was reported that values of contact angles ($\leq 90°$) relate to high hydrophilic surface, while contact angles ranged at 90°–150° correspond to low hydrophilic surface which is closed to the hydrophobic one, and contact angel's values > 150° are corresponding to super-hydrophobic surface [54]. The static water contact angles of various CA (PVA/Dex) NFs (M_{19}–M_{22}) scaffolds are drawn in Fig. 3b. Un-cross-linked (PVA/Dex) NFs were regarded as hydrophilic materials, due to their high surface hydrophilicity, where un-cross-linked NFs of M_{18} exposed remarked hydrophilic surface toward water droplets with a contact angle value of zero. Thus, CA-cross-linked scaffolds were adopted as a strategy to improve the surface morphological stability and to avoid the loss of fibrous-structure of mats upon contacting with water molecules. The water contact angle of NFs increased dramatically with increasing CA concentration. As observed, the water contact angles of NFs of M_{19}, M_{20}, M_{21} and M_{22} scaffolds were monitored at 45°, 58°, 70° and 92°, respectively (Fig. 3b). The contact angles of CA-cross-linked NFs increased with corresponding somewhat high wettability of NFs or increasing dextran contents in mats.

3.3.4 Swelling Ratio of NFs

Swelling of the dressing materials is one of the most important conditions and should be clarified and adjusted. Swelling ratio (%) indicates that the dressing can absorb wound exudates during the healing process and should be a balance between exudates absorption and microbial growth round/in wound core or area. The swelling results of CA-cross-linked PVA/Dex NFs as a function of NFs compositions in terms of dextran and CA different conditions are shown in Fig. 4. Generally, it noticed that the addition of CA reduced significantly the swelling rate (%) of PVA/Dex nanofibers, and the recorded swelling ratio of CA-cross-linked PVA/Dex nanofibers sharply decreased from 2800, 1500 and 1000%, when CA concentration increased (3, 5 and 10%, w/w), respectively, after 12 h of swelling. On the contrary, increasing the concentration of dextran increased clearly the swelling ratio (%) of PVA/Dex nanofibers, where the recorded swelling ratio were 600, 1200 and 1400% when dextran concentration increased as 5, 10 and 20%, w/w, respectively, after 12 h of swelling. According these findings, swelling results of NFs are ascribed to the increase in the CA concentration and increases in the cross-linking degree of NFs which results in the significant decrease in the swelling ratio of NFs. However, the increase in dextran contents in NFs decreased cross-linking degree of NFs which in term increases the entire swelling ratio of NFs.

3.3.5 Protein Adsorption of NFs

The blood biocompatibility of NFs and the interaction and activation of platelets adhered to the immune system are estimated by the extent of plasma proteins adsorbed on their surface. The adsorbed proteins of electrospun CA-cross-linked PVA/Dex NFs, as a function of different concentrations of both dextran and CA, are studied in Fig. 5a. Generally, protein adsorption % values of NFs increased gradually with

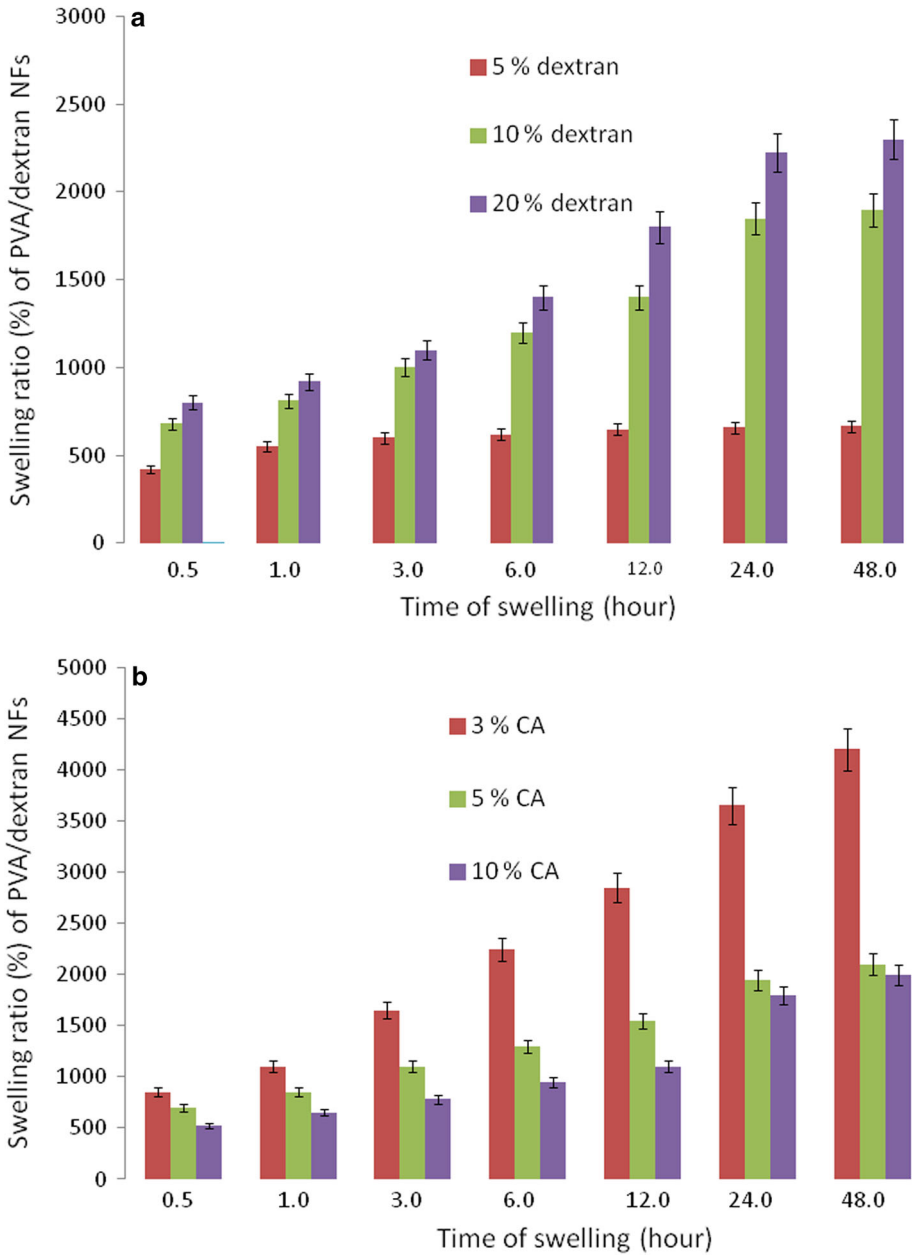

Fig. 4 Swelling ratio (%) of CA-cross-linked PVA–Dex NFs scaffolds as a function of **a**: different dextran concentrations (5, 10 and 20% w/w) and **b**: different CA cross-linker concentrations (3, 5 and 10%, w/w) (mean ± SD, $n = 3$, $P \leq 0.05$)

either increasing dextran contents and with decreasing CA cross-linker concentration in NFs. For example, PVA/Dex NFs cross-linked with CA of 3% showed the highest amount of adsorbed protein % on its surface of ~ 95%, due to its high hydrophilic surface of NFs, as previous confirmed by results of contact angle and swelling ratio. In addition, the protein adsorption capacity is reduced to ~ 60%, when increasing CA concentration to 10% CA. The protein adsorption capacity grows with the increase in the dextran concentration, where the protein adsorption capacity of PVA–Dex NFs was ~ 55% and ~ 90% for dextran contents in NFs of 5 and 20 (%, w/w). These results are consistent with our pervious results reported by Kamoun et al. [29].

3.3.6 Profile-Controlled Release of NFs

Effective dressing biomaterials for wound healing purposes require optimum drug loading with sustained and control the drug release profile at desired site. The released ampicillin from CA-cross-linked PVA/Dex NFs with different CA concentrations (1, 3, 5 and 10%, w/w) is presented in Fig. 5b. As seen, rapid initial burst effect or released ampicillin ~ 25% during the first 30 min of release was only observed with low cross-linked NFs (i.e., 1 and 3%, w/w of CA). However, the high cross-linked NFs with 5 and 10% w/w of CA do not show any initial burst release behavior. Notably, the low cross-linked NFs (i.e., 1%, w/w CA) released almost 95%

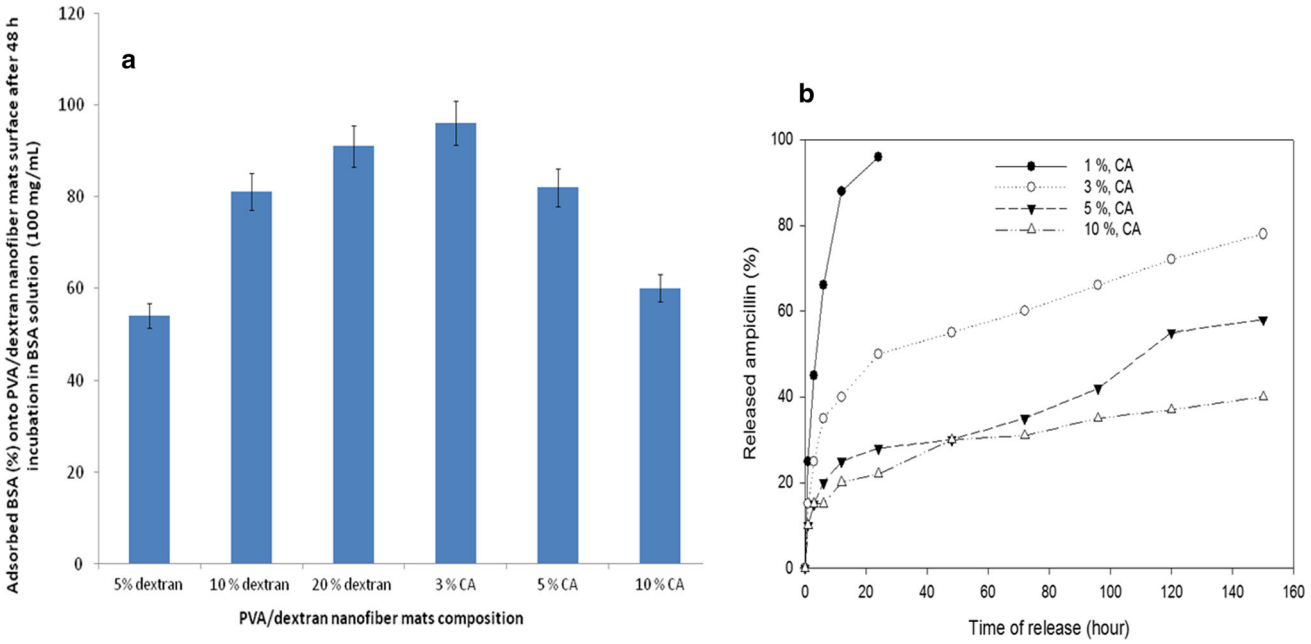

Fig. 5 **a** Protein adsorption (%) onto the surface of CA-cross-linked PVA–Dex NFs scaffolds, as a function on different dextran concentrations (5, 10 and 20% w/w) and different CA cross-linker concentrations (3, 5 and 10%, w/w) (mean ± SD, $n = 3$, $P \leq 0.05$); **b** in vitro profile release of sodium ampicillin from CA-cross-linked PVA–Dex NFs, as a function of different CA concentrations (1, 3, 5 and 10%, w/w)

of total loaded ampicillin after 24 h, compared to other high cross-linked NFs with 5 and 10%, w/w of CA which offered a sustained released reached to 45 and 25% released ampicillin after 150 h, respectively. These results indicate that high cross-linked NFs throughout using high CA concentrations showed a sustained profile release behavior and no initial burst release found, compared to the low cross-linked NFs. This concludes that the cross-linking degree of NFs influenced markedly on the released drug behavior of NFs.

3.4 In Vitro Bioevaluation Tests

3.4.1 Antimicrobial Activity of NFs Against Multidrug-Resistant Pathogens In Vitro

The microbial infection played clinically an energetic role in the wound healing process. As healing time and patient recovery time were prolonged, then the cost of the health service was raised for protecting the damaged skin from cellular dehydration and angiogenesis [5, 6]. So, previous reports focused on coating the wound dressings with antimicrobial materials to kill the skin clinical pathogens and detect its antagonism spectrum width [7, 8]. Many studied reported some hydrogels which were designed by natural or synthetic antimicrobial materials or compounds to prevent clinical bacterial infections, such as *S. aureus and P. aeruginosa,* which considered dangerous pathogens that potentially prevent the healing process and may lead the patient to death [3–6]. Ideal wound dressings should be fabricated using a transparent form, stimulated the healing and absorbed the exudates without produced skin injures [12–14]. Furthermore, the industrial production line of the wound dressings should be dependent on low-priced materials to reduce the total cost of the large-scale production [1–4]. Also, to fabricate a promising wound dressing, other properties should be accompanied such as antimicrobial efficacy against isolated clinical pathogens to prevent the formation of pathogens biofilm [5–7]. Recently, valuables challenges were found from the clinical application view which should be overcome since it will minimize the selling for the formulated hydrogels, such as producing hydrogels that have a proficient antimicrobial efficacy against both isolated clinical pathogens and the multidrug resistances pathogens [8, 9].

Until now, limited reports were studied the antimicrobial activities against multidrug-resistant microbes; so, in this report the designed hydrogels were assessed as an antimicrobial agent against multidrug-resistant bacteria and fungi (Fig. 6) to evaluate statistically its antagonistic effects in vitro (Table 4). Notably, the lowest cross-linked NFs with 1% CA (G4 disks) inhibited only the fungal cells (*C. albicans*, 5.7 ± 0.6 mm) but other tested bacterial pathogens resist it. Additionally, NFs cross-linked with 5% CA and the highest dextran concentration used 20%, w/w (G3 disks) and inhibited the growth of *S. aureus* (11.7 ± 1.5 mm), followed by *P. aeruginosa* (8.5 ± 1 mm) and *S. pyogenes* (5 ± 1 mm), except

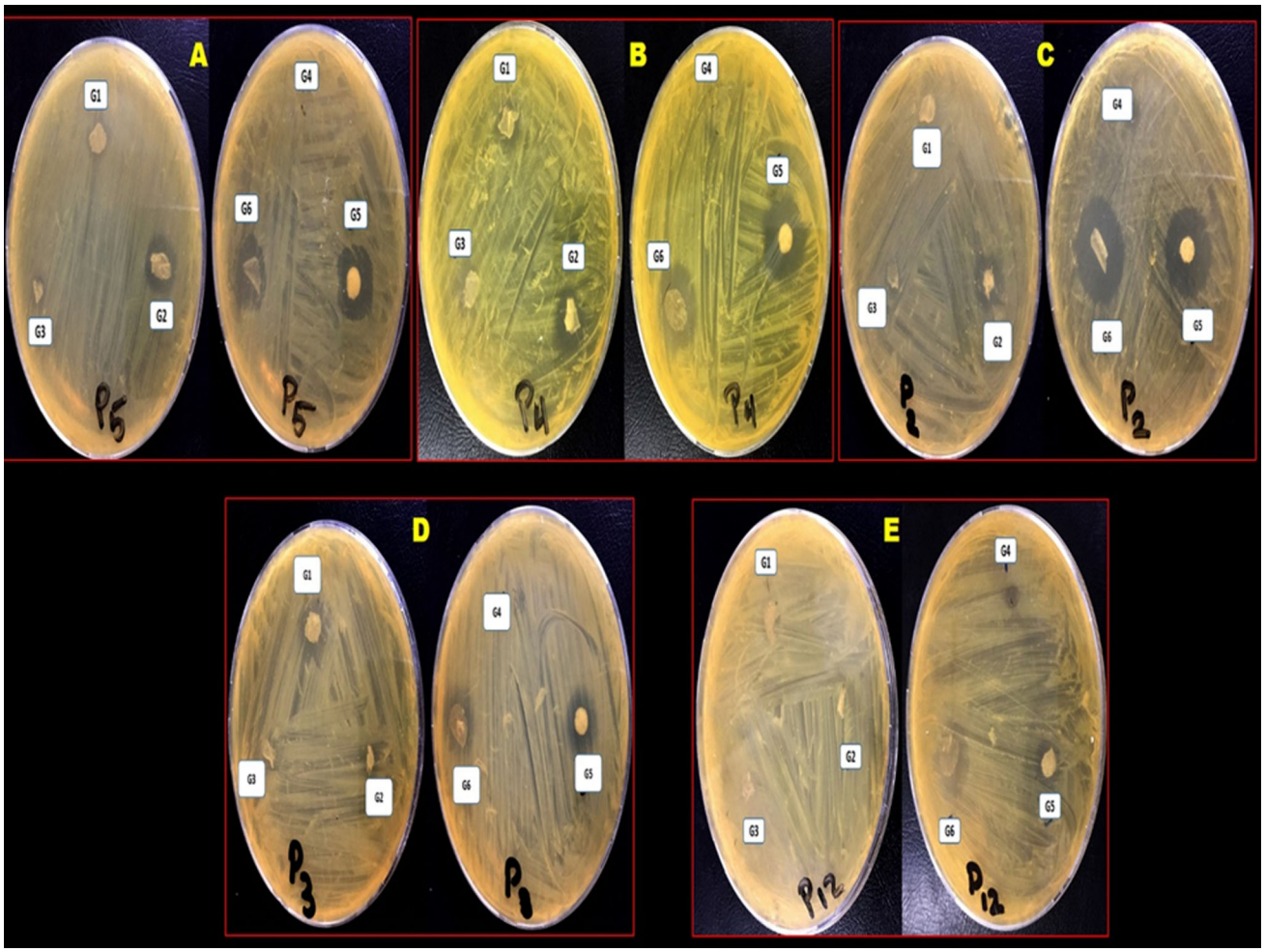

Fig. 6 Antagonistic efficacy of the formulated NFs against some multidrug-resistant human pathogens. The formulated hydrogels codes as G1: 10% PVA: 10% dextran: 5% CA, G2: 10% PVA: 5% dextran: 5% CA, G3: 10% PVA: 20% dextran: 5% CA, G4: 10% PVA: 10% dextran: 1% CA, G5: 10% PVA: 10% dextran: 3% CA and G6: 10% PVA: 10% dextran: 10% CA. The tested multidrug-resistant pathogens coded as **A**: *Staphylococcus aureus (gram-positive),* **B**: *Streptococcus pyogenes (gram-positive),* **C**: *Pseudomonas aeruginosa (gram-negative)*, **D**: *Klebsiella pneumoniae (gram-negative)* and **E**: *Candida albicans* (fungal cells)

Table 4 Disk diffusion assay of the formulated hydrogels (G1: 10% PVA: 10% dextran: 5% CA, G2: 10% PVA: 5% dextran: 5% CA, G3: 10% PVA: 20% dextran: 5% CA, G4: 10% PVA: 10% dextran: 1% CA, G5: 10% PVA: 10% dextran: 3% CA and G6: 10% PVA: 10% dextran: 10% CA against multidrug-resistant human pathogens to detect statistically the maximum inhibition halo/inhibition zones (mm ± SD)

Formulated NFs codes	Multidrug-resistant human pathogens				
	Gram-positive bacteria		Gram-negative bacteria		Fungal cells
	Staphylococcus aureus	*Streptococcus pyogenes*	*Pseudomonas aeruginosa*	*Klebsiella pneumoniae*	*Candida albicans*
G1	10.0 ± 1.0	9.0 ± 1.0	12.8 ± 1.0	13.5 ± 2.9	R
G2	10.0 ± 6.2	12.5 ± 0.6	5.7 ± 2.5	12 ± 1.4	R
G3	11.7 ± 1.5	5.0 ± 1.0	8.5 ± 1.0	R	R
G4	R	R	R	R	5.7 ± 0.6
G5	15.68 ± 2.06	9.4 ± 2.3	13.3 ± 1.7	15.3 ± 0.67	9.5 ± 1.3
*G6	18.0 ± 1.5	16.3 ± 1.0	14.5 ± 1.0	21.5 ± 1.0	17.8 ± 2.2

Values are means of three replicas. All results are highly significant ($P < 0.05$) using one-way analysis of variance (ANOVA). S.D: Standard deviation. R: Resistance, *: means the strong formulated hydrogel that produced the highest inhibition zone

that *K. pneumoniae* and *C. albicans* were grown in the presence of NFs. Furthermore, the strong antagonistic efficacy was recorded in the case of NFs cross-linked with 10% CA (G6 disks). Thus, the growth of all tested multidrug-resistant human pathogens were inhibited as shown in this orderliness: *K. pneumoniae* (21.5 ± 1 mm), *S.aureus* (18 ± 1.5 mm), *C. albicans* (17.8 ± 2.2 mm), *S. pyogenes* (16.3 ± 1 mm) and *P. aeruginosa* (14.5 ± 1 mm), individually. Finally, these results revealed that tested NFs cross-linked with 10% CA (G6 disks) were considered as promising candidate, which possessing antagonistic efficacy against different multidrug-resistant pathogens so it will use for treating and healing wounds proficiently. All these findings indicate that cross-linked NFs with high CA concentrations or containing high contents of dextran in NFs inhibited most tested multidrug-resistant pathogenic microbes, owing to the antimicrobial characteristics of dextran as previously reported by Kamoun et al. [29, 40].

3.4.2 Cytotoxicity Assay of NFs

The viability of *HFB-4* cells against prepared CA-cross-linked (PVA/Dex) NFs was estimated using MTT assay to determine the viability enhancement effect of NFs at various doses. Our results indicate that prepared NFs at high concentrations of dextran promote the proliferation of *HFB-4* cells in a high concentration-dependent manner, compared to NFs containing high concentrations of CA cross-linker after 24 and 48 h of cell exposure, as shown in Fig. 7. This can be referred to similarity of architecture between the extracellular matrix and NFs scaffolds which induce and promote the cell proliferation and adhesion [54]. M_{19}, M_{20} and M_{21} (*supplementary data*, Table 3), NFs recorded high cell viability (%) at concentration of 0.25 and 0.5 mg/ml of NFs on *HFB-4* cells (around 110–125%). The high cell proliferation might be owing to the combined effect between PVA and dextran that are considered wound accelerating agents, as mentioned above. As shown in Fig. 7, *HFB-4* melanocyte cells cannot grow well on the presence of high concentration of tested NFs with 2 mg/ml after adding for 48 h, particularly with tested NFs containing high CA-cross-linked disks by 1, 3 and 5% (w/w) of CA (M_{19}, M_{20} and M_{21}), respectively. After 48 h of culturing, NFs contents high CA cross-linker concentration M_{22}, M_{23} and M_{24} showed clearly a cytotoxic effect in a dose dependent manner than those treated with NFs disks containing high dextran concentrations of M_{19}, M_{20} and M_{21} NFs. Thus, the addition of dextran into NFs composition allowed markedly growing the cells proliferation regardless the used high concentration; however, using CA as cross-linker for NFs with high concentration greater than 3% (w/w) hindered significantly the cell viability of *HFB-4* cells.

3.4.3 Wound Closure (%) of NFs

For a proper wound closure process, normal fibroblasts must migrate and proliferate to the wound scratch bed in a well manner, during the cell proliferation process, wherever they promote the secretion of extracellular matrix (ECM) of the granulation tissue [55]. *HFB-4* cells are a human skin fibroblast cells derived from a normal skin *melanocyte*. Fibroblasts enhance secretion of collagen, neo-angiogenesis and re-epithelialization [56]. In this concern, a wound closure assay was carried out using *HFB-4* fibroblasts to estimate the proliferation and the migration manners in response to different applied NFs. Figures 8 and 9 show the micrographs morphology alteration and kinetics of wound closure process and, the wound healing efficiency of the tested NFs, respectively, at concentration of 0.5 mg/ml of NFs after incubation for 24 and 48 h as compared to untreated control cells. In general, all prepared NFs have the ability to accelerate the rate of gap closure (%) after treatment for 24 and 48 h, compared to control. NFs codes M_{19}, M_{21} and M_{24} showed the highest percentages of wound healing for scratched *HFB-4* cells with clear observed healing process (Figs. 8 and 9). PVA NFs promoted absorption of wound exudates and provide regeneration of cells and tissues due to their biocompatibility, safety and oxygen permeability [57, 58]. Notably, NFs containing high concentrations of CA (5% w/w) and moderated concentration of dextran showed adequate wound closure even after premature treatment time. This result could be ascribed to the fact that CA might decrease the microbes growing and accelerates the wound closure process; however, high contents of dextran in NFs keep the wettability of wound and a somewhat delay the healing process.

4 Conclusions

In conclusion, electrospun CA-cross-linked PVA/Dex NFs were fabricated by electrospinner to report the optimized concentration of nanofiber fabrication. The optimized CA-PVA/Dex NFs were examined by SEM investigation and other instrumental characterization, e.g., FTIR analysis, mechanical stability, TGA thermographs, water contact angle, swelling ratio % and protein adsorption. The influence of CA concentration and dextran blending on NFs properties was studied in detail. CA concentration 10% (W/W) was used as chemical cross-linker via esterification reaction of PVA NFs and significantly improved mechanical and thermal stability of NFs from premature dissociation and prolonged the sustained released sodium ampicillin for more than 6 days. On the contrary, blending of dextran into PVA NFs notably enhanced the surface wettability/hydrophilicity, swelling ability and protein adsorption of NFs. In addition, dextran blending improved significantly the antimicrobial

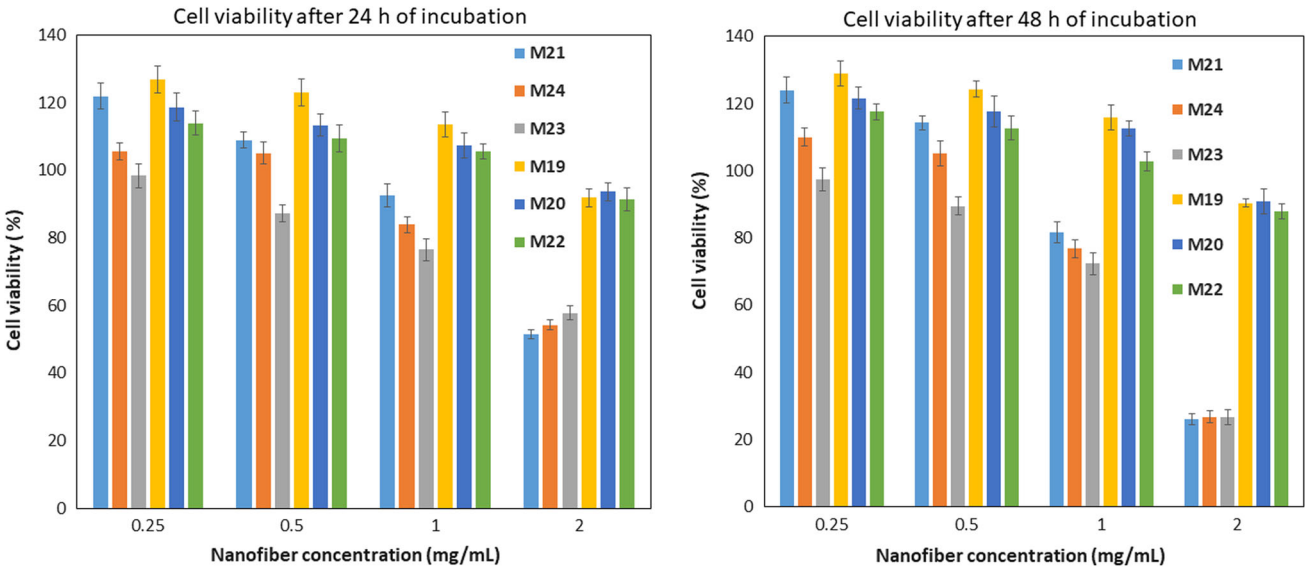

Fig. 7 Cytotoxicity test by MTT assay of CA-cross-linked PVA–Dex NFs as a function of different CA concentrations, using HFB-4 viability % after culturing for 24 h (left) and 48 h (right)

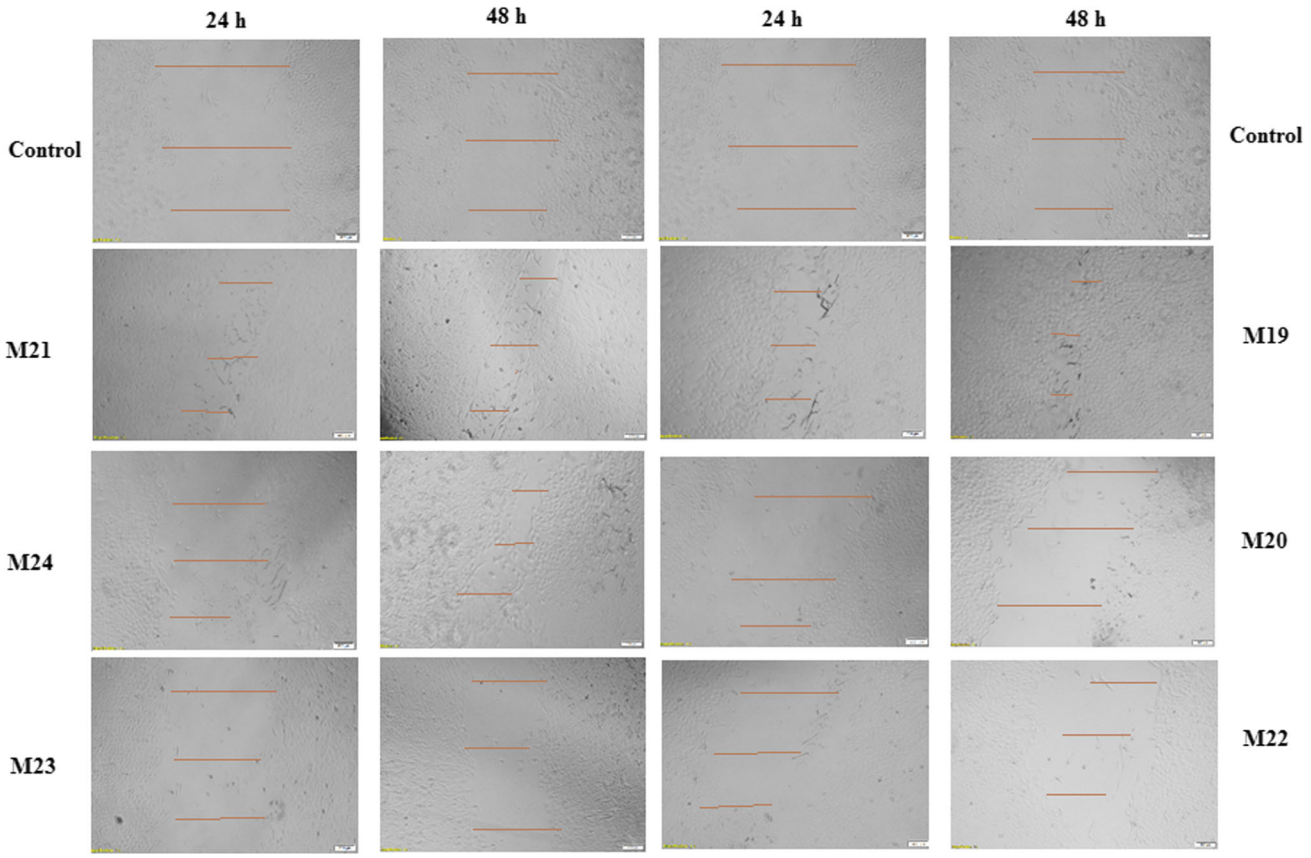

Fig. 8 In vitro HFB-4 cells migration after incubation for 24 and 48 h cultured onto CA-cross-linked PVA–Dex NFs as a function of different CA concentration codes (M_{19}, M_{20}, M_{21}, M_{22}, M_{23} and M_{24}) (scale bar is 500 μm for each image). The red bars indicate the measured distances used in calculating the wound closure (%)

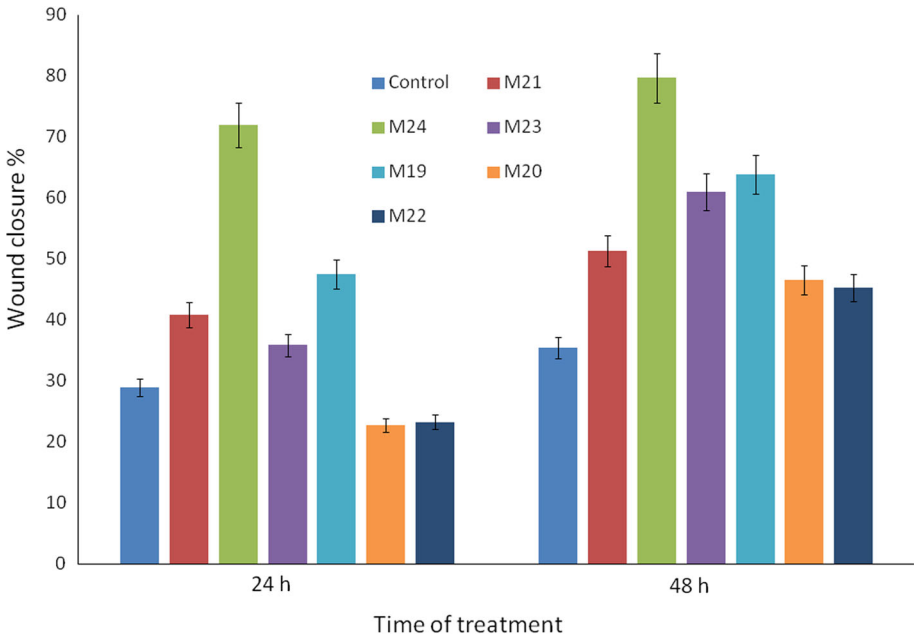

Fig. 9 In vitro wound closure (%) of CA-cross-linked PVA/Dex NFs scaffolds using NFs concentration of 0.5 mg/ml after 24 and 48 h of treatment time, as compared to untreated control cells

activity, cell viability and in vitro wound closure (%) of NFs mats. These findings are referring to the ability of using electrospun CA-cross-linked PVA/Dex NFs as good candidate biomaterials for different biomedical applications, in particular wound dressing applications.

Supplementary Information The online version contains supplementary material available at https://doi.org/10.1007/s13369-022-06856-9.

Acknowledgements Authors would like to acknowledge the financial support of this work by STDF-Egypt through Project ID 28987.

Authors' contribution E.S.K. was involved in study design, supervision and reviewing the original draft; M.S.E. was responsible for methodology and writing the original draft; E.A.K. had contributed to study suggestion, conceptualization, validation, resources, writing, review and editing the original draft, data curation and supervision; H.M.A.S. and A.M.S. carried out supervision; S.H.E.-M. took part in methodology, formal analysis, data curation and writing the original draft; and E.E.-F. participated in methodology, formal analysis and data curation. All authors approve the publication of the manuscript in the current version.

Funding Open access funding provided by The Science, Technology & Innovation Funding Authority (STDF) in cooperation with The Egyptian Knowledge Bank (EKB).

Declarations

Conflict of interests None.

References

1. Andreu, V.; Mendoza, G.; Arruebo, M.; Irusta, S.: Smart dressings based on nanostructured fibers containing natural origin antimicrobial, anti-inflammatory, and regenerative compounds. Materials **8**, 5154–5193 (2015)
2. Gao, Z.H.; Deng, C.J.; Xie, Y.-Y.; Guo, X.L.; Wang, Q.Q.; Liu, L.Z.; Lee, W.H.; Li, S.A.; Zhang, Y.: Pore-forming toxin-like protein complex expressed by frog promotes tissue repair. Faseb J. **33**, 1–14 (2018)
3. Wang, F.; Hu, S.; Jia, Q.; Zhang, L.: Advances in electrospinning of natural biomaterials for wound dressing. J. Nanomater. **2020**, 1–14 (2020) (**Article ID 8719859**)
4. Chen, S.; Liu, B.; Carlson, M.A.; Gombart, A.F.; Reilly, D.A.; Xie, J.: Recent advances in electrospun nanofibers for wound healing. Nanomedicine **12**, 1335–1352 (2017)
5. Zahedi, P.; Rezaeian, I.; Ranaei-Siadat, S.O.; Jafari, S.H.; Supaphol, P.: A review on wound dressings with an emphasis on electrospun nanofibrous polymeric bandages. Polym. Adv. Technol. **21**, 77–95 (2010)
6. Chen, D.W.; Liao, J.Y.; Liu, S.J.; Chan, E.C.: Novel biodegradable sandwich-structured nanofibrous drug-eluting membranes for repair of infected wounds: an in vitro and in vivo study. Int. J. Nanomed. **7**, 763–771 (2012)
7. Wang, S.X.; Yap, C.C.; He, J.T.; Chen, C.; Wong, S.Y.; Li, X.: Electrospinning: a facile technique for fabricating functional nanofibers for environmental applications. Nanotechnol. Rev. **5**, 51–73 (2016)

8. Mayet, N.; Choonara, Y.E.; Kumar, P.; Tomar, L.K.; Tyagi, C.; Du Toit, L.C.; Pillay, V.A.: Comprehensive review of advanced biopolymeric wound healing systems. J. Pharm. Sci. **103**, 2211–2230 (2014)
9. Akia, M.; Rodriguez, C.; Materon, L.; Gilkerson, R.; Lozano, K.: Antibacterial activity of polymeric nanofiber membranes impregnated with Texas sour orange juice. Eur. Polym. J. **115**, 1–5 (2019)
10. Prakash, C.; Sukumar, N.; Ramesh, P.; Kumar, S.K.S.: Development and characterization of wound dressing material coated with natural extracts of curcumin, Aloe vera and chitosan solution enhanced with rhEGF (REGEN-D-TM). J. Nat. Fibers **18**(12), 2019–2032 (2020)
11. Zou, P.F.; Lee, W.H.; Gao, Z.Q.; Qin, D.; Wang, Y.X.; Liu, J.; Sun, T.Y.; Gao, Y.Y.: Wound dressing from polyvinyl alcohol/chitosan electrospun fiber membrane loaded with OH-CATH30 nanoparticles. Carbohydr. Polym. **232**, 115786 (2020)
12. Pathalamuthu, P.; Siddharthan, A.; Giridev, V.R.; Victoria, V.; Thangam, R.; Sivasubramanian, S.; Savariar, V.; Hemamalini, T.: Enhanced performance of Aloe vera incorporated chitosan-polyethylene oxide electrospun wound scaffold produced using novel Spirograph based collector assembly. Int. J. Biol. Macromol. **140**, 808–824 (2019)
13. Nitti, P.; Gallo, N.; Natta, L.; Scalera, F.; Palazzo, B.; Sannino, A.; Gervaso, F.: Influence of nanofiber orientation on morphological and mechanical properties of electrospun chitosan mats. J. Healthc. Eng. **2018**, 3651480 (2018)
14. de Souza Simoes, L.; Madalena, D.A.; Pinheiro, A.C.; Teixeira, J.A.; Vicente, A.A.; Ramos, O.L.: Micro- and nano bio-based delivery systems for food applications: in vitro behavior. Adv. Colloid Interface Sci. **243**, 23–45 (2017)
15. Aytac, Z.; Kusku, S.I.; Durgun, E.; Uyar, T.: Encapsulation of gallic acid/cyclodextrin inclusion complex in electrospun polylactic acid nanofibers: release behavior and antioxidant activity of gallic acid. Mater. Sci. Eng. C Mater. Biol. Appl. **63**, 231–239 (2016)
16. Tong, H.W.; Wang, M.: Electrospinning of fibrous polymer scaffolds using positive voltage or negative voltage: a comparative study. Biomed. Mater. **5**, 054110 (2010)
17. Sandri, G.; Miele, D.; Faccendini, A.; Bonferoni, M.C.; Rossi, S.; Grisoli, P.; Taglietti, A.; Ruggeri, M.; Bruni, G.; Vigani, B.: Chitosan/glycosaminoglycan scaffolds: the role of silver nanoparticles to control microbial infections in wound healing. Polymers **11**, 1207 (2019)
18. Nayak, R.; Padhye, R.; Kyratzis, I.; Truong, Y.B.; Arnold, L.: Recent advances in nanofiber fabrication techniques. Text. Res. J. **82**, 129–147 (2012)
19. El-Hadi, A.M.; Al-Jabri, F.Y.: Influence of electrospinning parameters on fiber diameter and mechanical properties of poly(3-hydroxybutyrate) (PHB) and polyanilines (PANI) blends. Polymers **8**, 97 (2016)
20. Reneker, D.H.; Chun, I.: Nanometre diameter fibres of polymer, produced by electrospinning. Nanotechnolology **7**, 216–223 (1996)
21. Zahedi, P.; Rezaeian, I.; Ranaei-Siadat, S.O.; Jafari, S.H.; Supaphol, P.: A review on wound dressings with an emphasis on electrospun nanofibrous polymeric bandages. Polym. Adv. Technol. **21**, 77–95 (2009)
22. Mwiiri, F.K.; Daniels, R.: Electrospun nanofibers for biomedical applications. In: Shegokar, R. (Ed.) Delivery of Drugs, pp. 53–74. Elsevier, Tuebingen (2020)
23. Kai, D.; Liow, S.S.; Loh, X.J.: Biodegradable polymers for electrospinning: towards biomedical applications. Mater. Sci. Eng. C **45**, 659–670 (2014)
24. Zhong, S.P.; Zhang, Y.; Lim, C.T.: Tissue scaffolds for skin wound healing and dermal reconstruction. Wiley Interdiscip. Rev. Nanomed. Nano. **2**, 510–525 (2010)
25. Ignatova, M.; Rashkov, I.; Manolova, N.: Drug-loaded electrospun materials in wound-dressing applications and in local cancer treatment. Mater. Sci. Eng. **10**, 469–483 (2013)
26. Jiang, T.; Carbone, E.J.; Lo, K.W.H.; Laurencin, C.T.: Electrospinning of polymer nanofibers for tissue regeneration. Prog. Polym. Sci. **46**, 1–24 (2015)
27. Gajra, B.; Pandya, S.S.; Vidyasagar, G.; Rabari, H.; Dedania, R.R.; Rao, S.: Poly vinyl alcohol hydrogel and its pharmaceutical and biomedical applications: a review. Int. J. Pharm. Res. **4**, 2026 (2012)
28. Gaaz, T.S.; Sulong, A.; Akhtar, M.N.; Kadhum, A.A.H.; Mohamad, A.B.; Al-Amiery, A.: Properties and applications of polyvinyl alcohol, halloysite nanotubes and their nanocomposites. Molecules **20**, 22833–22847 (2015)
29. Kamoun, E.A.; Chen, X.; Eldin, M.S.M.; Kenawy, E.R.: Crosslinked poly(vinyl alcohol) hydrogels for wound dressing applications: a review of remarkably blended polymers. Arab. J. Chem. **8**, 1–14 (2015)
30. Augustine, R.; Hasan, A.; Nath, V.K.Y.; Thomas, J.; Augustine, A.; Kalarikkal, N.; AlMoustafa, A.E.; Thomas, S.: Electrospun polyvinyl alcohol membranes incorporated with green synthesized silver nanoparticles for wound dressing applications. J. Mater. Sci. Mater. Med. **29**, 163 (2018)
31. Saeed, S.M.; Mirzadeh, H.; Zandi, M.; Barzin, J.: Designing and fabrication of curcumin loaded PCL/PVA multi-layer nanofibrous electrospun structures as active wound dressing. Prog. Biomater. **6**, 39–48 (2017)
32. Kim, J.A.; Choi, H.G.: Development of polyvinyl alcohol–sodium alginate gel-matrix-based wound dressing system containing nitrofurazone. Int. J. Pharm. **359**, 79–86 (2008)
33. Levic, S.; Rac, V.; Manojlovic, V.; Rakic, V.; Bugarski, B.; Flock, T.; Krzyczmonik, K.E.; Nedovi, N.: Limonene encapsulation in alginate-poly(vinyl alcohol). Procedia Food Sci. **1**, 1816–1820 (2011)
34. Zhao, L.; Mitomo, H.; Zhai, M.; Yoshii, F.; Nagasawa, N.; Kume, T.: Synthesis of antibacterial PVA/CM chitosan blend hydrogels with electron beam irradiation. Carbohyd. Polym. **53**, 439–446 (2003)
35. Kenawy, E.; Kamoun, E.A.; Mohy Eldin, M.S.; El-Meligy, M.A.: Physically crosslinked poly(vinyl alcohol)- hydroxyethyl starch blend hydrogel membranes: synthesis and characterization for biomedical applications. Arab. J. Chem. **7**(3), 372–380 (2014)
36. Huang, X.; Brazel, C.S.: Review On the importance and mechanisms of burst release in matrix-controlled drug delivery systems. J. Control. Rel. **73**, 121–136 (2001)
37. Cascone, M.G.; Maltinti, S.; Barbani, N.: Effect of chitosan and dextran on the properties of poly(vinylalcohol) hydrogels. J. Mater. Sci. Mater. Med. **10**, 431–435 (1999)
38. El-Salmawi, K.M.: Gamma radiation-induced crosslinked PVA/Chitosan blends for wound dressing. J. Macromol. Sci. Part A Pure Appl. Chem. **44**, 541–545 (2007)
39. Hago, E.E.; Li, X.: Interpenetration polymer network hydrogels based on gelatin and PVA by biocompatible approaches: synthesis and characterization. Adv. Mater. Sci. Eng. **2013**, 1–8 (2013) (**Article ID 328763**)
40. Kamoun, E.A.; Loutfy, S.; Hussien, Y.; Kenawy, E.: Recent advances in PVA-polysaccharide based hydrogels and electrospun nanofibers in medical applications: a review. Int. J. Biol. Macromol. **187**, 755–768 (2021)
41. Salim, S.A.; Kamoun, E.A.; et al.: mercaptopurine-loaded sandwiched tri-layered composed of electrospun polycaprolactone/poly (methyl methacrylate) nanofibrous scaffolds as anticancer carrier with antimicrobial and antibiotic features: sandwich configuration nanofibers, release study and in vitro bioevaluation tests. Int. J. Nanomed. **16**, 6937–6955 (2021)
42. Salim, S.A.; Kamoun, E.A.; et al.: Novel oxygen-generation from electrospun nanofibrous scaffolds with anticancer properties:

synthesis of PMMA-conjugate PVP-H_2O_2 nanofibers, characterization, and in vitro bio-evaluation tests. RSC Adv. **11**, 19978 (2021)
43. Sidebotham, R.L.: Dextrans. Adv. Carbohydr. Chem. Biochem. **30**, 371–444 (1974)
44. Kamoun, E.A.; Menzel, H.: Crosslinking behavior of dextran modified with hydroxyethyl methacrylate upon irradiation with visible light- effect of concentration, coinitiator type, and solvent. J. Appl. Polym. Sci. **117**, 3128–3138 (2010)
45. Hwang, M.R.; Kim, J.O.; Lee, J.H.; Kim, Y.; Kim, J.H.; Chang, S.W.; Jin, S.G.; Kim, J.A.; Lyoo, W.S.; Han, S.S.; Ku, S.K.; Young, C.S.; Choi, H.G.: Gentamicin-loaded wound dressing with polyvinyl alcohol/dextran hydrogel, gel characterization and in vivo healing evaluation. AAPS PharmSciTech **11**, 1092–1103 (2010)
46. Rashedi, S.; Afshar, S.; Rostami, A.; Ghazalian, M.; Nazockdast, H.: Co-electrospun poly(lactic acid)/gelatin nanofibrous scaffold prepared by a new solvent system: morphological, mechanical and in vitro degradability properties. Int. J. Polym. Mater. Polym. Biomater. **8**, 545–553 (2021)
47. Ibrahim, H.M.; Klingner, A.: A review on electrospun polymeric nanofibers: production parameters and potential applications. Polym. Test. **90**, 106647 (2020)
48. Li, Y.; Zhu, J.; Cheng, H.; Li, G.; Cho, H.; Jiang, M.; Gao, Q.; Zhang, X.: Developments of advanced electrospinning techniques: a critical review. Adv. Mater. Technol. **6**, 2100410 (2021)
49. Mosmann, T.: Rapid colorimetric assay for cellular growth and survival, application to proliferation and cytotoxicity assays. J. Immunol. Methods **65**, 55–63 (1983)
50. Almahdy, O.; EL-Fakharany, E.M.; EL-Dabaa, E.; Ng, T.B.; Redwan, E.M.: Examination of the activity of camel milk casein against hepatitis C virus (genotype-4a) and its apoptotic potential in hepatoma and Hela cell lines. Hepat. Mon. **11**, 724–730 (2011)
51. Preet, R.; Mohapatra, P.; Sahu, S.K.; Choudhuri, T.; Wyatt, M.D.; Kundu, C.N.: Quinacrine has anticancer activity in breast cancer cells through inhibition of topoisomerase activity. J. Int. Cancer **130**, 1660–1670 (2011)
52. El-Lakany, S.A.; Abd-Elhamid, A.I.; Kamoun, E.A.; El-Fakharany, E.M.; Samy, W.M.; Elgindy, N.A.: α-Bisabolol-loaded cross-linked Zein nanofibrous 3D-scaffolds for accelerating wound healing and tissue regeneration in rats. Int. J. Nanomed. **14**, 8251–8270 (2019)
53. Jiang, H.; Zhao, P.; Zhu, K.: Fabrication and characterization of zeinbased nanofibrous scaffolds by an electrospinning method. Macromol. Biosci. **7**(4), 517–525 (2007)
54. Mariggiò, M.A.; Cassano, A.; Vinella, A.; Vincenti, A.; Fumarulo, R.; Lo, M.L.; Maiorano, E.; Ribatti, D.; Favia, G.: Enhancement of fibroblast proliferation, collagen biosynthesis and production of growth factors as a result of combining sodium hyaluronate and aminoacids. Int. J. immunopathol. Pharmacol. **22**(2), 485–492 (2009)
55. Coelho, D.S.; Veleirinho, B.; Alberti, T.; Maestri, A.; Yunes, R.; Dias, P.F.; Maraschin, M.: Electrospinning Technology: Designing Nanofibers Toward Wound Healing Application, Nanofibers-From Preparation to Applications, Chapter 1–20. IntechOpen, Rijeka (2018)
56. Yeh, C.-J.; Chen, C.-C.; Leu, Y.-L.; Lin, M.-W.; Chiu, M.-M.; Wang, S.-H.: The effects of artocarpin on wound healing: in vitro and in vivo studies. Rep. **7**(1), 15599 (2017)
57. Jannesari, M.; Varshosaz, J.; Morshed, M.; Zamani, M.: Composite poly (vinyl alcohol)/poly (vinyl acetate) electrospun nanofibrous mats as a novel wound dressing matrix for controlled release of drugs. Int. J. Nanomed. **6**, 993–1003 (2011)
58. Shalumon, K.; Anulekha, K.; Nair, S.V.; Nair, S.; Chennazhi, K.; Jayakumar, R.: Sodium alginate/poly (vinyl alcohol)/nano ZnO composite nanofibers for antibacterial wound dressings. Int. J. Biol. Macromol. **49**(3), 247–254 (2011)